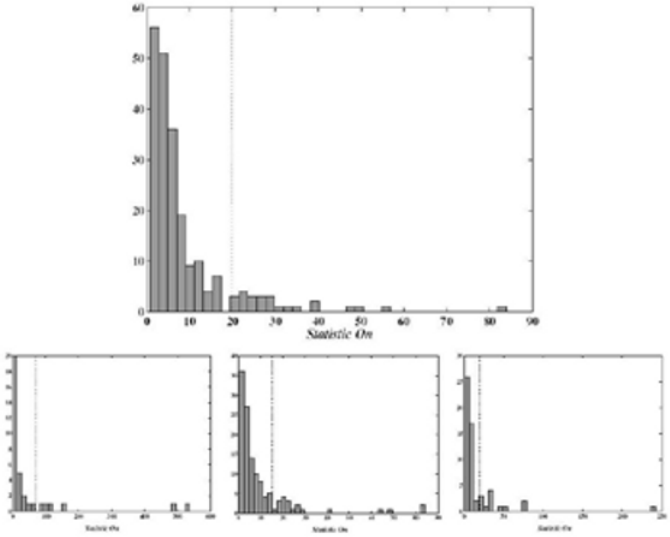


Fig.2: (Top figure): Histogram of statistic O_n for the complete SET dataset. (Bottom row figures): Histograms of statistic O_n for each of the tumour groups in the SET dataset: (left): Low grade gliomas; (centre): High grade malignant tumours; (right): Meningiomas. The selected thresholds of *outlierness* are represented as vertical dotted lines.

Id	*Tum*	*Dis*	*Artifact-relat. outl.*					
			noi	wat	ali	bas	pol	edd
10335	G1(a2)	X						
11052*	G1(a2)		X					
11087*	G1(a2)			X				
10060	G1(oa)		X					
10069	G1(oa)				X			
10450	G1(oa)	X						
10179	G1(od)	X						
10135*	G2(gl)					X		
10172*	G2(gl)			X		X		
10354*	G2(gl)						X	
10421*	G2(gl)			X				
11024*	G2(gl)			X				
10055	G2(me)		X					
10244*	G3(mm)	X						
10375	G3(mm)		X					
10381*	G3(mm)			X				
10390*	G3(mm)						X	
10393*	G3(mm)		X			X	X	
11283*	G3(mm)		X	X			X	X

Id	*Tum*	*Artifacts*					
		noi	wat	ali	bas	pol	edd
Low grade gliomas (G1)							
$\emptyset$							
High grade malignant (G2)							
10021*	gl						
10358*	gl					X	
10200*	gl					X	
11390	gl			X			
10168*	gl						
11098*	gl						
11076*	me				X		
10352*	me				X		
11377*	me						
Meningiomas (G3)							
10160*	mm						
11090*	mm						
11073*	mm					X	
10069	mm						
10390*	mm					X	
11378*	mm				X		
10375	mm	X				X	
11149*	mm						

Fig.3: (Left): Outlier characterization of the complete SET dataset. Columnwise, *Id* is an anonymized case identifier; star superscripts indicate that there are artifacts that do not preclude the expert's correct interpretation of the case. *Tum* refers to tumour type (see labels in section 2). *Dis* identifies *distinct outliers*. Six types of artifacts were found: *noi* stands for noise; *wat*, for bad water signal suppression; *ali*, for alignment; *lin*, baseline; *pol*, for the polispiculated effect; and *edd* for eddy currents. (Right): *Class outlier* characterization by groups of tumours. Label description as in (left).

23

Multiproject-Multicenter evaluation of automatic brain tumor classification by Magnetic Resonance Spectroscopy

J. M. Garcia-Gomez[1], J. Luts[2], M. Julià-Sapé[3,4], P. Krooshof[5], S. Tortajada[1], J. Vicente[1], W. Melssen[5], E. Fuster-García[1], I. Olier[4], G. Postma[5], D. Monleón[6,3], À. Moreno-Torres[7], J. Pujol[8], A.-P. Candiota[3,4], M. Martínez-Bisbal[3,9], J. Suykens[10], L. Buydens[11], B. Celda [12], S. Van Huffel[13], C. Arús[14], M. Robles[15]

[1]IBIME-Itaca, Universidad Politecnica de Valencia, Valencia, Spain, [2]Department of Electrical Engineering (ESAT), Research Division SCD, Katholieke Universiteit Leuven, Leuven, Belgium, [3]CIBER de Bioingeniería, Biomateriales y Nanomedicina, Zaragoza, Spain, [4]Departament de Bioquímica i Biologia Molecular, Universitat Autònoma de Barcelona, Cerdanyola del Vallès, Spain, [5]Institute for Molecules and Materials, Radboud University, Nijmegen, Netherlands, [6]Fundación de Investigación del Hospital Clínico Universitario de Valencia, Valencia, Spain, [7]Research Department, Centre Diagnòstic Pedralbes, Esplugues de Llobregat, Spain, [8]Institut d'Alta Tecnologia-PRBB, CRC Corporació Sanitària, Barcelona, Spain, [9]Departamento de Química-Física, Universidad de Valencia, Valencia, Spain, [10]Universiteit Leuven, Department of Electrical Engineering (ESAT), Research Division SCD, [11]University, Institute for Molecules and Materials the Netherlands (Gelderland), [12]CIBER de Bioingeniería, Biomateriales y Nanomedicina; Universitat de Valencia, Departamento de Química-Física, [13]Katholieke Universiteit Leuven, Department of Electrical Engineering (ESAT), Research Division SCD, [14]Universitat Autònoma de Barcelona, Departament de Bioquímica i Biologia Molecular; CIBER de Bioingeniería, Biomateriales y Nanomedicina, [15]Universidad Politécnica de Valencia, IBIME-Itaca

Purpose/Introduction: Automatic brain tumor classification by Magnetic Resonance Spectroscopy (MRS) has been under development for more than a decade. Nonetheless, to our knowledge, there are no published evaluations of predictive models with unseen cases that are subsequently acquired in different centers. The development of the multicenter eTUMOUR project (2004-2009), which builds upon previous expertise from the INTERPRET project (2000-2002), which is also multicenter, has allowed such an evaluation to take place.

Subjects and Methods: A set of 275 pairwise classifiers for Glioblastoma (GBM), Meningioma (MEN), Metastasis (MET), and Low-Grade Glial (LGG) diagnoses were inferred based on 211 Single Voxel Short TE 1H INTERPRET MR spectra obtained at 1.5T (PRESS or STEAM, 20-32 ms) and automatically pre-processed. Afterwards, the classification models were tested with 97 spectra, which were subsequently compiled during eTUMOUR. Peak Integration (PI), Region of Interest (190), Peak height of typical resonances (PPM), Principal Component Analysis (PCA), Independent Component Analysis (ICA) and Wavelets (WAV) were applied for feature extraction. Parametric discriminant analysis (LDA), kernel-based methods (Support Vector Machines, SVM and Least-Squares Support Vector Machines, LSSVM), local classifiers (KNN) and neural networks (Multilayer Perceptron, MLP and Bi-Directional Kohonen Networks, BDK) were the methods applied for classification.

Results: In our results, based on subsequently acquired spectra, accuracies of around 90% were achieved for most of the pairwise discrimination problems. The exception was for the Glioblastoma versus Metastasis discrimination which was below 78%. Figure 1 shows the scatter plot of the performance of the 275 classifiers measured in Balanced Error Rate (BER) estimated

by the Independent Test (IT) set consisting of new eTUMOUR cases and the BER estimated by the Cross Validation (CV) using the INTERPRET cases. BER(IT)=BER(CV) is represented by the solid-blue line and the trend of the (BER(CV)<0.2,BER(IT)<0.3) region is indicated by the black-dashed line. Table 1 shows the best result for each pairwise classification problem.

Discussion/Conclusion: The prediction of the tumor type based on the PR analysis of in-vivo MRS is possible using classifiers developed from previously acquired data, in different hospitals with different instrumentation under the same acquisition protocols. This automated classification systems may find application for assisting in the diagnosis of new brain tumor cases. It can also be used for the quality control of future multicenter MRS databases.

Figure1

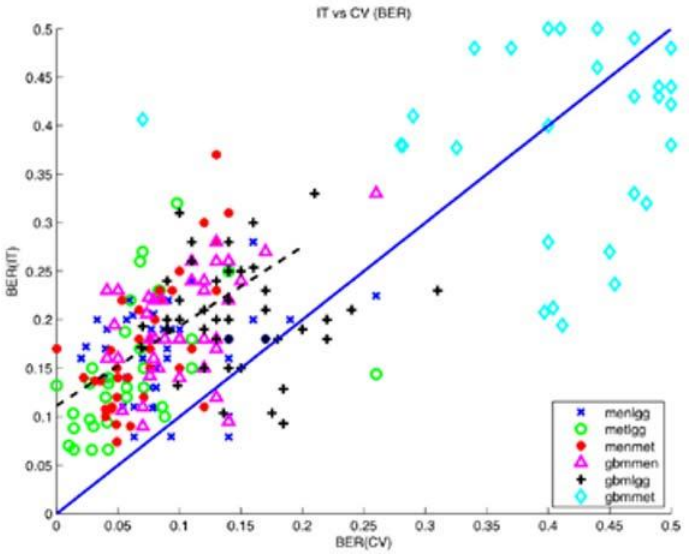


Table1

The best results for the six pairwise classification problems.

Problem	Feature Extraction	Classification method	Balanced Error Rate
GBM vs MEN	190	MLP	0.09
GBM vs MET	PI	LDA	0.21
GBM vs LGG	PI	LSSVM	0.09
MEN vs MET	PCA	MLP	0.07
MEN vs LGG	ICA/WAV/PI/PPM	LDA/LSSVM	0.11
MET vs LGG	PI	LDA/MLP/BDK	0.07

9 Teaching Session I

2:20 pm - 3:50 pm *Auditorio 2*

MRI Artefacts and Fast Imaging

24a

Recognition of and how to avoid artefacts in MRI

P. M. Jakob;
Department of Physics, Experimental Physics 5, Würzburg, Germany.

An MRI artifact is any undesired feature which appears in an image which is not present in the original object. MR artifacts arise due to data inconsistencies in the acquired *k*-space data, which after Fourier Transform results influence the fidelity with which the object is reproduced. Image artifacts appear in various fashions with the result that e.g. the object being imaged may appear ghosted, distorted, shifted in the image space, or have a non-uniform intensity or not be there at all. Most common artifacts can be grouped roughly into three general categories, namely (1) MR hardware related artifacts, (2) artifacts, where the object being sampled is in itself the artifact source, and (3) user related artifacts. However, almost any not-hardware-related image artifact can be removed or attenuated by a proper acquisition strategy or reconstruction method or a combination of both. Some of these artifacts affect the MR image quality very noticable, or bring just a few pixels out of balance, but in the worst case scenario they may be confused with pathology, leading to a wrong diagnosis with major consequences. This course will review some of the most important sources of artifacts (neglecting scanner related hardware artifacts) and techniques to combat the resulting artifacts.

24b

Ultrafast imaging (Parallel imaging)

K. Scheffler;
Department of Radiology, Division of Radiological Physics, Basel, Switzerland.

Several methods have been developed to speed up the imaging process. A simple method is to reduce TR. For gradient echo sequences this leads to a very rapid train of consecutive excitation pulses. If properly adjusted (constant or zero dephasing within excitations) a steady state (SSFP) between excitation, dephasing, relaxation, and polarization is established. In SSFP TR of just several milliseconds is possible and thus used for time-critical applications such as MR angiography, cardiac or perfusion imaging. As a consequence of rapid excitation SSFP sequences in general exhibit a mixed T1 and T2 contrast. For spin echo sequences a simple reduction of TR immediately leads to horrible image artifacts caused by the rapid repetition of the excitation-refocusing module. However, repetition of just the refocusing pulse results in the well known RARE (FSE, TSE) sequence (as for SSFP, constant dephasing is required within refocusing pulses). Imaging speed of RARE is comparable to SSFP as long as SAR is not an issue.

A further increase of imaging speed is possible with single-shot sequences such as EPI, or a combination of RARE or SSFP with EPI. In EPI, k-space is acquired after one single excitation either by rectangular or spiral (or random) trajectories. Imaging speed is only limited by gradient performance and peripheral nerve stimulation. In contrast to RARE or SSFP, EPI is sensitive to field inhomogeneities due to its low readout bandwidth (in phase